





Recrystallization in string-fluid complex plasmas

E. Joshi ^{1,*}, M. Y. Pustyl'nik ¹, M. H. Thoma,² H. M. Thomas ¹ and M. Schwabe ^{1,3}

¹*Institut für Materialphysik im Weltraum, Deutsches Zentrum für Luft- und Raumfahrt, 51147 Köln, Germany*

²*I. Physikalisches Institut, Justus-Liebig Universität Gießen, 35392 Gießen, Germany*

³*Deutsches Zentrum für Luft- und Raumfahrt (DLR), Institut für Physik der Atmosphäre, 82234 Oberpfaffenhofen, Germany*



(Received 21 January 2022; revised 29 November 2022; accepted 16 January 2023; published 2 March 2023)

Complex plasmas, i.e., low-temperature plasmas containing suspensions of solid microparticles, exhibit electrorheological properties which are manifested by the formation of stringlike clusters (SLCs) in microgravity experiments. It is thought that SLCs form due to a long-range effective attraction between the particles under the influence of a directed ion flow. We performed molecular dynamics (MD) simulations of negatively charged microparticles with positive model wakes to mimic the effect of ion flow in experiments, and achieved SLC formation without long-range attraction between the microparticles. We show that long-range-reduced repulsion was enough to obtain the SLCs similar to the experiments and found that the simulations with the long-range attraction became unstable due to particle accelerations. Destruction and recrystallization of the stringlike structure was also studied experimentally using the Plasmakristall-4 facility on board the International Space Station, and the experimental findings were compared to those from three-dimensional MD simulations. We found excellent qualitative agreement between simulation and experiment when recrystallization was simulated using an interparticle potential without effective long-range attraction.

DOI: [10.1103/PhysRevResearch.5.L012030](https://doi.org/10.1103/PhysRevResearch.5.L012030)

Electrorheological fluids are electrically insulating fluids with polarizable micrometer-sized particles embedded in them [1–3]. When an electric field is applied to these systems, the microparticles align along the field and drastically change the rheological properties of the system, such as shear viscosity and dynamic modulus, giving rise to a wide range of potential applications [4].

The other class of systems with electrorheological properties are complex plasmas [5–7]. Complex plasmas are ionized gases with suspensions of micrometer-sized “dust” particles embedded in them [8,9]. These microparticles become highly negatively charged, and their interparticle interactions are governed by a shielded Coulomb (or Yukawa) interaction potential. The subsystem of these microparticles can become strongly coupled, thus, allowing it to be used to model generic classical condensed-matter phenomena. Electrorheology in complex plasmas is observed on the application of an external electric field: the microparticles align themselves in stringlike clusters (SLCs) [10–13]. The electric field causes an ion flow that deforms the ion cloud around the microparticles and leads to a buildup of excess positive charge behind them. This positively charged region, known as an “ion wake,” is responsible for modifying the interparticle potential and, thus, leads to the stringlike microparticle arrangement. SLCs in conventional electrorheological fluids form due to long-range

(compared to a characteristic distance, in our case the distance of the wake to the particle) interparticle attraction [14], and it is widely assumed that this is also the case in complex plasmas [15–20].

The presence of long-range attraction would, however, naturally result in the appearance of a characteristic interparticle distance inside the SLCs equal to the position of the bottom of the potential well in the interaction potential. At the same time, in the direction orthogonal to the external electric field, the interparticle distance should be determined by the balance of interparticle repulsion and confinement forces. Recent experiments in the Plasmakristall-4 (PK-4) facility suggest that the interparticle distances inside the SLCs are very close to the interstring distances [12,13], which questions the necessity of long-range attraction for the formation of the SLCs. In this Letter, we use a new approach to molecular dynamics (MD) simulations [6] to show for the first time that this long-range attraction is not necessary for string formation, and that simply reducing the repulsion along a given axis is sufficient to form SLCs aligned in that direction.

For this purpose, we studied the formation and recrystallization of SLCs in complex plasmas using both simulations and experiments under microgravity conditions in the PK-4 facility on board the International Space Station [21].

We used an experimental procedure similar to Refs. [22–24]. The heart of the PK-4 setup is a cylindrical glass plasma chamber of 3-cm diameter in which a direct current (DC) glow discharge is created (see the Supplemental Material [25] for a sketch of the experimental setup). In our particular experiment, argon gas at the pressure of 11 Pa was used as working gas. At the beginning of the experiment, 3.38- μm diameter melamine formaldehyde microspheres were introduced into the peripheral region of

*eshita.joshi@dlr.de

the chamber. A DC discharge of 0.5-mA current transported the microparticles into the working area. Once they became visible (due to the illumination by a laser sheet) by the centrally positioned cameras, the discharge regime was changed from the unipolar DC to polarity switching. In the polarity switching regime, the polarity of the active electrode was switched with the frequency of 500 Hz. This frequency is high enough for the microparticles to not react to the periodic variations of the electric field. In this way, the microparticles were trapped in the discharge chamber. At this frequency the ions can still follow the switching electric field and lead to the formation of wakes on both sides of the microparticles.

The suspension of trapped microparticles exhibited string-like structure similarly to Refs. [12,13]. In order to destroy the stringlike structure and observe further recrystallization, we switched off the discharge for some fractions of a second. This was long enough to destroy the structure of the system, whereas, the timescale for recrystallization was observed to be of the order of magnitude of a few seconds. We note that a similar “plasma-off” technique was used in Ref. [26] to determine the spatial profile of the manipulation laser intensity *in situ*. Before and after the recrystallization process, the suspension of microparticles was scanned in order to measure its three-dimensional (3D) structure. The velocity of the scan was 0.9 mm/s, and the scanning range was 14 mm. During the recrystallization, the position of the camera was static. Therefore, only two-dimensional (2D) information was available. This procedure was repeated several times at the same discharge conditions with the same microparticle suspension with different plasma-off durations. Since in all cases the behavior was similar, we concentrate in the following on a particular example with the plasma-off time of 0.3 s.

To process the experimental data, we used the sequence of video images from one of the PK-4 cameras. The field of view had a size of 1600×600 pixels and the frame rate of the video recording was 60 fps.

The 3D positions of the microparticles were determined from the scans using the algorithm described in Ref. [12]. For the 2D data obtained during the recrystallization, the 2D microparticle positions, and velocities could be determined in each image.

To simulate the experiment in 3D, we used the open source software the ‘Large-scale Atomic/Molecular Massively Parallel Simulator’ [27]. The main forces acting on the particles in the simulation are the interparticle force given by the Yukawa potential, the Langevin force due to the thermostat, and the Epstein damping due to the friction with the background gas.

Previous MD simulations of electrorheological complex plasmas mimic the effect of ions by using a wake potential to describe the interparticle interactions [28–30]. For our simulation, we modified the Yukawa potential by including two-point wake charges around each particle [6]. We positioned two wakes of charge $-w_c q$ (q is the microparticle charge) downstream and upstream the particle at a distance of r_w along the x axis. As a result, we expect to see SLCs aligned with the x axis. Our code for the custom modification to the potential can be found in Ref. [31]. The wake charge and distance are the two free parameters we can change to adjust the strength of the interparticle interactions in order to obtain

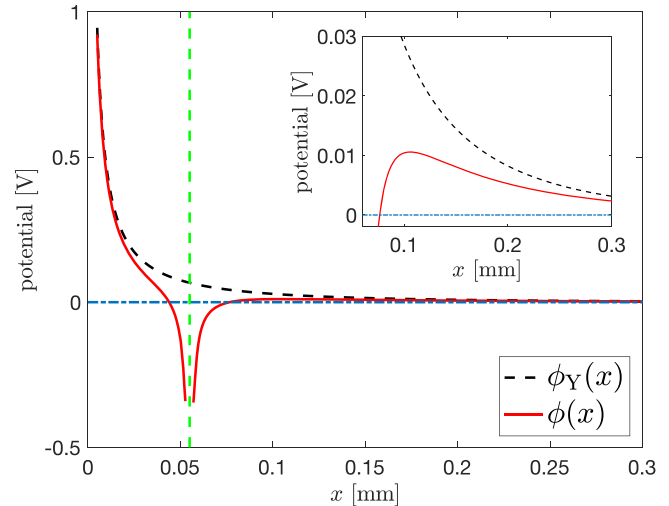


FIG. 1. Axial profiles of the pure Yukawa potential ϕ_Y and the total potential ϕ . The axis x coincides with the direction of \mathbf{r}_w . The location of the point wake with a charge of $-0.2q$ ($x = 0.055$ mm) is marked by a vertical dashed line. The inset shows the long-range tail of the interaction potential. The interaction potential appears to be repulsive at large distances. The repulsion is however significantly reduced compared to the Yukawa potential.

SLCs. This brings us to the model interaction potential we will use in the MD simulations: $\phi = \phi_Y + \phi_{w+} + \phi_{w-}$ with

$$\phi_Y = \frac{q}{4\pi\epsilon_0 r} \exp(-\kappa r), \quad (1)$$

$$\phi_{w\pm} = \frac{-w_c q}{4\pi\epsilon_0 |\mathbf{r} \mp \mathbf{r}_w|} \exp(-\kappa_{\text{eff}} |\mathbf{r} \mp \mathbf{r}_w|), \quad (2)$$

where r is the interparticle distance and

$$\kappa_{\text{eff}} = \sqrt{\frac{\kappa^2}{(1 + M_{\text{th}}^2 \cos^2 \zeta)} + \kappa_e^2}. \quad (3)$$

Here, M_{th} is the thermal mach number of the ions, ζ is the angle between the vector connecting the microparticles and the direction of the externally applied electric field (and, hence, the ion flow), κ is the inverse of the interparticle screening length, and κ_e determines the electron screening. The effective screening for the potential due to the wake is affected by the direction and speed of the ion flow.

The axial profiles of the interparticle interaction potentials used are plotted in Fig. 1. The Yukawa potential is shown with a black dashed line, whereas, the total potential ϕ is shown with a solid red line in Fig. 1. It can be clearly seen in the inset that the combined potential is not attractive after $x \approx 75$ μm and is instead repulsive at long distances. It should, however, be noted that the total potential is significantly less repulsive compared to the pure Yukawa potential.

Changing the wake charge changes the width of the potential well, and changing the wake distance moves the potential well along the x axis. The wider the potential well and the further away it is from the particle, the more the repulsion is reduced compared to Yukawa potential. Increasing the wake charge past a threshold led to the interparticle potential becoming attractive at long distances (see the Supplemental Material [25]). This caused strong acceleration of the particles

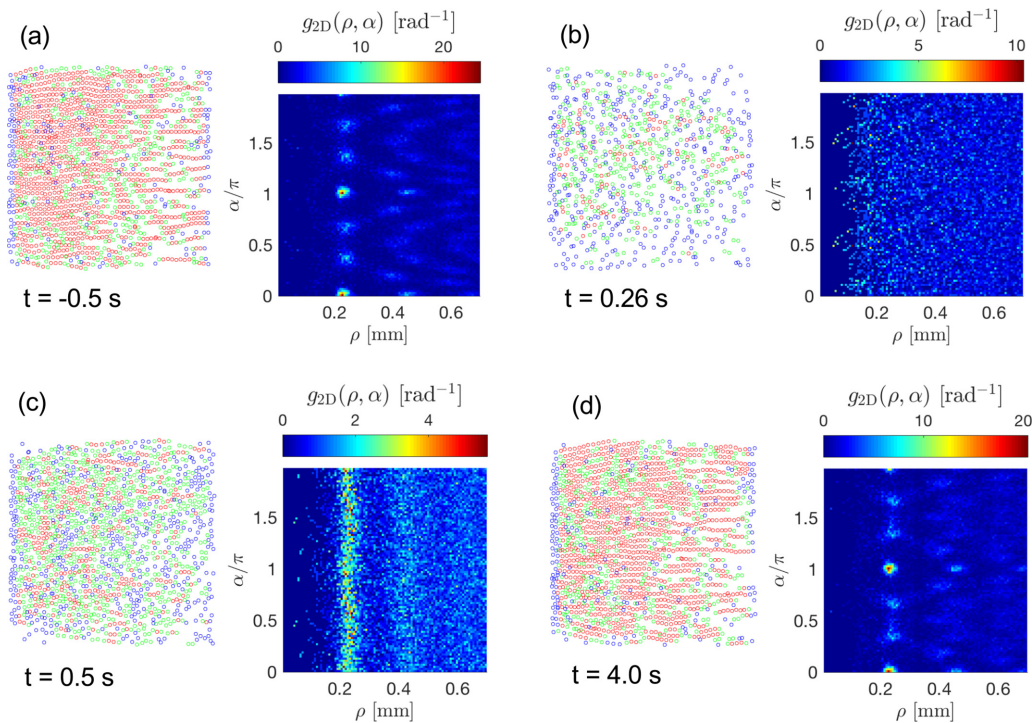


FIG. 2. Pairs of plots showing the number of string neighbors (left) and the pair correlation function (right) for the system at various times during the experiment. A particle is colored red if it has two string neighbors, green if it has one, and blue if it has none. It can be seen clearly that the structure in (a) at $t = -0.5$ s was destroyed completely by melting at $t = 0$ s in (b) at $t = 0.26$ s and was reformed fully by (d) at $t = 4$ s.

making the simulation unstable, consistent with the observations in previous simulations [6,28]. We found that the time taken to form the SLCs was very sensitive to r_w and w_c , and could be increased or decreased by changes to the potential well.

Below, we concentrate on an example simulation with $w_c = 0.2$ and $r_w = 55 \mu\text{m}$. The data used in the following analysis can be found in Ref. [32]. We first initialized the system at thermal equilibrium with a Yukawa potential, and then modified the interparticle potential to include positive charges and, thus, mimicked the wakes caused by the ion flow. We then induced crystallization by reducing the microparticle temperature from 1200 K to 300 K and waited for the system to form the SLCs. Once the system reached equilibrium, we simulated the plasma-off phase in the experiments by destroying the order in the system. This was performed by: (i) drastically reducing the particle charge, and (ii) increasing their temperature to 1200 K. After 0.3 s we reverted the changes, let the system relax back to equilibrium and reform the SLCs.

To perform the simulation, we used a time step of 10 μs and a data acquisition rate of 1000 fps. We used a simulation box with dimensions $4.5 \times 3 \times 3 \text{ mm}^3$. We generated microparticles with an interparticle distance of 227 μm and a Yukawa interparticle potential for particles with a charge of $q = -3481$ elementary charges [33] and a Debye length of 190 μm . We used a Langevin dynamics thermostat with an Epstein damping coefficient corresponding to argon gas at a pressure of 11 Pa. We also used periodic boundary conditions. By doing so, we assume that in our case the plasma density is low enough for the ion drag force acting on the microparticles

to not be sufficient to balance the electrostatic force. In this case, as shown in Refs. [34–36], the radial stability of the microparticle suspension can only be provided if the ambipolar electric field vanishes, and the ionization balance localizes. During the plasma-off time, the microparticle charge was set to $-10 e$ instead of zero since residual charges are found on microparticles in the afterglow [37]. However, this did not seem to be noticeably different from the simulations with zero residual charge.

A limitation of the simulation was that after the simulated recrystallization process, often a few particles got trapped in the potential well created by the wakes and as a result became attached to their neighbors. We hypothesize this occurred due to the particles moving past the small potential barrier due to either too large a time step or because they were suddenly and strongly repelled by other particles. We saw benefit from reducing the time step, but found no way to completely eliminate this effect.

In order to qualitatively characterize the 3D structure of the microparticle suspensions in both simulation and experiments, we used the 3D pair correlation function in spherical coordinates and its angular integrals [13]. The definition of these quantities is given in the Supplemental Material [25].

For the experimental 2D data obtained in the illuminated slab during the recrystallization process, we defined the pair correlation function in polar coordinates as follows:

$$g_{2D}(\rho, \alpha) = \frac{1}{\sigma_d N} \sum_{\substack{i,j=1 \\ i \neq j}}^N \frac{\delta(\rho_{i,j} - \rho) \delta(\alpha_{i,j} - \alpha)}{\rho}, \quad (4)$$

where $\rho_{i,j}$ and $\alpha_{i,j}$ are the length and polar angle of the vector connecting the particles i and j , respectively, whereas ρ and α are the current polar coordinates, N is the total number of particles in the considered system, and σ_d is the 2D density of particles in the image. The direction with $\alpha = 0$ corresponds to the axis of the plasma chamber.

The radial and angular widths of the string peaks in the correlations determined which neighbors of a particle formed an SLC together [13]. For the experimental data, the peaks in the 2D pair correlations $g_{2D}(\rho, \alpha)$ were used. For the simulated data, we relied on the 3D correlation functions (see the Supplemental Material [25]). Particles that lie inside the string peaks were identified as string neighbors [12,13]. We defined the ‘stringiness’ as the average number of string neighbors at any given time, and used it as a measure of the order in the system.

The 3D correlation functions for the experimental and simulated data are included in the Supplemental Material [25]. From this correlation analysis, we conclude that in the simulations as well as in the experiments, the suspensions of particles exhibit qualitatively similar stringlike order. Also, the order before and after the plasma off event is similar (but not exactly the same) in the experiment and in the simulations.

The evolution of the structure of the experimental suspension before and after the order was destroyed is shown in Fig. 2 using 2D data. We suppose (both for experimental and for simulated data) that the plasma is switched off at time $t = 0$. Two strong peaks are visible in Fig. 2(a) at $\alpha = \pi$ and $\alpha = 0$ corresponding to the direction of the SLC formation in the experiment. It can be seen in Fig. 2(b) that the structure was completely destroyed and eventually reformed to reach equilibrium [Fig. 2(d)]. The destruction of the order in the simulated system is confirmed by the 3D correlation analysis in the Supplementary Material [25].

The variation of the stringiness of the system with time for both experimental and simulated data is plotted in Fig. 3. The figure shows remarkable similarity between the experimental and the simulated data. Both the experimental and simulated systems were at equilibrium before the plasma was turned off and returned to their equilibrium states after the plasma was turned on again. The velocities in Fig. 3(b) for both experiment and simulation rise suddenly once the plasma is turned on again and then decay to equilibrium in a few milliseconds. This happens since the microparticles lose their charge quickly once the plasma is turned off in the experiment, which allows some microparticles to approach each other very closely. When their charges are restored, the particles rapidly shoot away from each other giving rise to the peak in velocity in both the experimental and simulation plot immediately after the plasma is turned on again.

We can see from Fig. 3(a) that the shape of the stringiness in both the simulation and experiment is qualitatively very similar, and the time taken to reach equilibrium is also very similar. We can also see from Fig. 3 that the change in stringiness happens a lot slower than the change in particle velocity. This suggests that SLC formation depends on mechanisms other than just heating or cooling of the particles. After being cooled down, the particles have to diffuse to their equilibrium positions in the SLCs. Below, we give a rough estimation of this diffusion time.

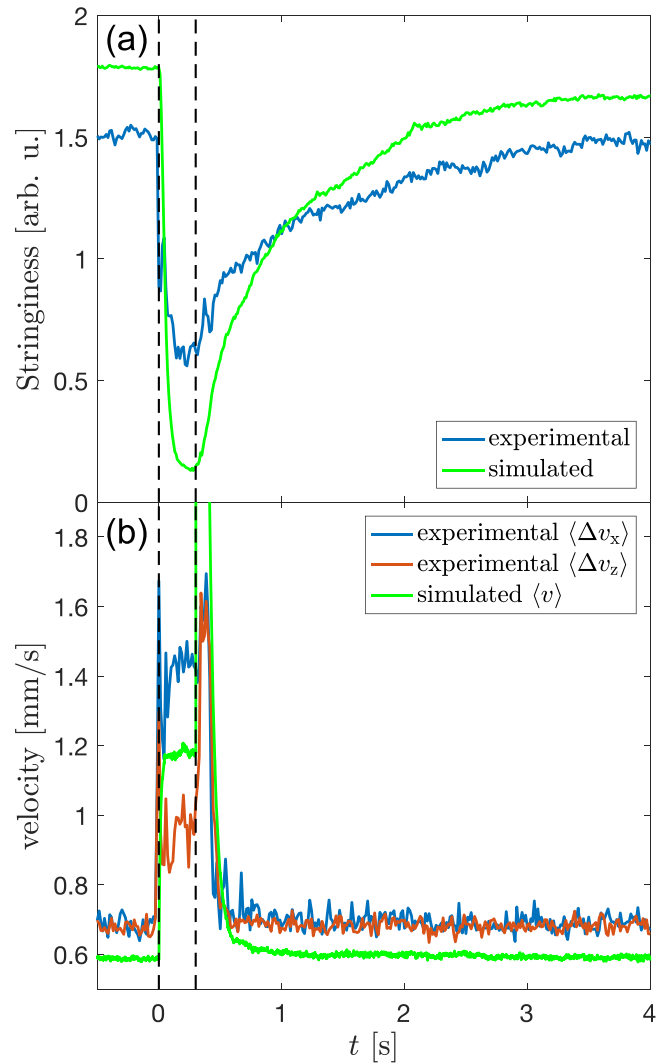


FIG. 3. Time variation of the (a) stringiness of the microparticles, (b) average chaotic microparticle velocities in the simulations and in the experiment. For the experimental data, the differences between the local drift velocity and velocity of each microparticle were considered.

Under the assumption of weak coupling, the diffusion coefficient can be expressed as $D = lv_T/3$, where v_T is the thermal velocity of the particles, and l is their mean free path. In its turn, $l = (\sigma n_d)^{-1}$, where n_d is the microparticle number density, and σ is the cross-sectional area.

Since the velocities of the microparticles are very small, the cross-section, σ , will be mainly determined by the geometry of the shielding ion cloud which can be represented as an ellipsoid with the semiaxes κ^{-1} and $\kappa^{-1} + r_w$. Then, σ can be estimated as an average of the areas of the three projections of this ellipsoid,

$$\sigma = \frac{1}{3} [\pi \lambda_D^2 + 2\pi \lambda_D (\lambda_D + r_w)], \quad (5)$$

where $\lambda_D = \kappa^{-1}$. This results in $D = 1.6 \times 10^{-8} \text{ m}^2 \text{ s}^{-1}$ for the parameters used in the simulation. Finally, the relaxation time can be defined as the time required for a particle to diffuse the distance of the order of average interparticle

distance d : $t_{\text{diff}} \sim d^2/D \approx 2.46$ s, which is consistent with the experimental observations and simulation data.

To conclude, microparticles in complex plasmas often form structures with stringlike order when an external electric field is applied. Until now, the formation of the SLCs has been attributed to a long-range effective attraction between the microparticles. We found that this process is not necessarily a consequence of attraction between the particles as assumed in many previous papers, but rather a consequence of the reduced repulsion in the direction of the dipole-dipole interactions. We performed and simulated “recrystallization” experiments in which the stringlike order in a stable microparticle suspension was destroyed by shortly switching the plasma off. After that, the suspension relaxed to the initial order within seconds.

Excellent qualitative agreement between the experimental results and the results of the simulation suggests that reducing the repulsion along a given direction in the interaction potential is a sufficient condition for the formation of

SLCs in complex plasmas. The estimations also show that the relaxation time is determined by the diffusion of the microparticles to their equilibrium positions in the SLCs.

We gratefully acknowledge the joint ESA-Roscosmos experiment “Plasmakristall-4” on board the International Space Station and cosmonaut A. Ivanishin for performing the experiment. We thank R. A. Syrovatka, A. V. Zobnin, A. M. Lipaev, and A. D. Usachev at the Joint Institute of High Temperatures for their assistance in the preparation, execution, and analysis of the experiment and their support of the publication of this Letter. We also thank P. Born, H. Heuer, and the referees for careful reading of the Letter and their valuable feedback. We acknowledge funding of this work in the framework of the Nachwuchsgruppenprogramm im DLR-Geschäftsbereich Raumfahrt. This work was partly supported by DLR under Grant No. 50WM2044 and by DLR/BMWi Grant No. 50WM1441.

-
- [1] P. M. Adriani and A. P. Gast, A microscopic model of electrorheology, *Phys. Fluids* **31**, 2757 (1988).
- [2] T.-j. Chen, R. N. Zitter, and R. Tao, Laser Diffraction Determination of the Crystalline Structure of an Electrorheological Fluid, *Phys. Rev. Lett.* **68**, 2555 (1992).
- [3] U. Dassanayake, S. Fraden, and A. van Blaaderen, Structure of electrorheological fluids, *J. Chem. Phys.* **112**, 3851 (2000).
- [4] Y. D. Liu and H. J. Choi, Electrorheological fluids: Smart soft matter and characteristics, *Soft Matter* **8**, 11961 (2012).
- [5] A. V. Ivlev, G. E. Morfill, H. M. Thomas, C. R ath, G. Joyce, P. Huber, R. Kompaneets, V. E. Fortov, A. M. Lipaev, V. I. Molotkov, T. Reiter, M. Turin, and P. Vinogradov, First Observation of Electrorheological Plasmas, *Phys. Rev. Lett.* **100**, 095003 (2008).
- [6] M. Schwabe, S. A. Khrapak, S. K. Zhdanov, M. Y. Pustyl'nik, C. R ath, M. Fink, M. Kretschmer, A. M. Lipaev, V. I. Molotkov, A. S. Schmitz, M. H. Thoma, A. D. Usachev, A. V. Zobnin, G. I. Padalka, V. E. Fortov, O. F. Petrov, and H. M. Thomas, Slowing of acoustic waves in electrorheological and string-fluid complex plasmas, *New J. Phys.* **22**, 083079 (2020).
- [7] C. Dietz, J. Budak, T. Kamprich, M. Kretschmer, and M. H. Thoma, Phase transition in electrorheological plasmas, *Contrib. Plasma Phys.* **61**, e202100079 (2021).
- [8] V. Fortov, A. Ivlev, S. Khrapak, A. Khrapak, and G. Morfill, Complex (dusty) plasmas: Current status, open issues, perspectives, *Phys. Reports* **421**, 1 (2005).
- [9] G. E. Morfill and A. V. Ivlev, Complex plasmas: An interdisciplinary research field, *Rev. Mod. Phys.* **81**, 1353 (2009).
- [10] L. W rner, C. R ath, V. Nosenko, S. K. Zhdanov, H. M. Thomas, G. E. Morfill, J. Schablinski, and D. Block, String structures in driven 3D complex-plasma clusters, *Europhys. Lett.* **100**, 35001 (2012).
- [11] S. Mitic, B. A. Klumov, S. A. Khrapak, and G. E. Morfill, Three dimensional complex plasma structures in a combined radio frequency and direct current discharge, *Phys. Plasmas* **20**, 043701 (2013).
- [12] M. Y. Pustyl'nik, B. Klumov, M. Rubin-Zuzic, A. M. Lipaev, V. Nosenko, D. Erdle, A. D. Usachev, A. V. Zobnin, V. I. Molotkov, G. Joyce, H. M. Thomas, M. H. Thoma, O. F. Petrov, V. E. Fortov, and O. Kononenko, Three-dimensional structure of a string-fluid complex plasma, *Phys. Rev. Res.* **2**, 033314 (2020).
- [13] S. Mitic, M. Y. Pustyl'nik, D. Erdle, A. M. Lipaev, A. D. Usachev, A. V. Zobnin, M. H. Thoma, H. M. Thomas, O. F. Petrov, V. E. Fortov, and O. Kononenko, Long-term evolution of the three-dimensional structure of string-fluid complex plasmas in the PK-4 experiment, *Phys. Rev. E* **103**, 063212 (2021).
- [14] C. Park and R. E. Robertson, Alignment of particles by an electric field, *Mater. Sci. Eng.* **257**, 295 (1998).
- [15] M. Nambu, S. V. Vladimirov, and P. K. Shukla, Attractive forces between charged particulates in plasmas, *Phys. Lett. A* **203**, 40 (1995).
- [16] S. V. Vladimirov and O. Ishihara, On plasma crystal formation, *Phys. Plasmas* **3**, 444 (1996).
- [17] A. V. Ivlev, M. H. Thoma, C. R ath, G. Joyce, and G. E. Morfill, Complex Plasmas in External Fields: The Role of Non-Hamiltonian Interactions, *Phys. Rev. Lett.* **106**, 155001 (2011).
- [18] O. Arp, J. Goree, and A. Piel, Particle chains in a dilute dusty plasma with subsonic ion flow, *Phys. Rev. E* **85**, 046409 (2012).
- [19] H. Jung, F. Greiner, O. H. Asnaz, J. Carstensen, and A. Piel, Exploring the wake of a dust particle by a continuously approaching test grain, *Phys. Plasmas* **22**, 053702 (2015).
- [20] V. Yaroshenko and M. Pustyl'nik, Possible mechanisms of string formation in complex plasmas at elevated pressures, *Molecules* **26**, 308 (2021).
- [21] M. Y. Pustyl'nik, M. A. Fink, V. Nosenko, T. Antonova, T. Hagl, H. M. Thomas, A. V. Zobnin, A. M. Lipaev, A. D. Usachev, V. I. Molotkov, O. F. Petrov, V. E. Fortov, C. Rau, C. Deysenroth, S. Albrecht, M. Kretschmer, M. H. Thoma, G. E. Morfill, R. Seurig, A. Stettner *et al.*, Plasmakristall-4: New complex (dusty) plasma laboratory on board the International Space Station, *Rev. Sci. Instrum.* **87**, 093505 (2016).
- [22] C. Knapek, D. Samsonov, S. Zhdanov, U. Konopka, and G. E. Morfill, Structural Properties and Melting of 2D-Plasma Crystals, *New Vistas in Dusty Plasmas: Fourth International*

- Conference on the Physics of Dusty Plasmas*, AIP Conf. Proc. No. 799 (AIP, Melville, NY, 2005), p. 231.
- [23] C. A. Knapek, D. Samsonov, S. Zhdanov, U. Konopka, and G. E. Morfill, Recrystallization of a 2D Plasma Crystal, *Phys. Rev. Lett.* **98**, 015004 (2007).
- [24] V. Nosenko, S. K. Zhdanov, A. V. Ivlev, C. A. Knapek, and G. E. Morfill, 2D Melting of Plasma Crystals: Equilibrium and Nonequilibrium Regimes, *Phys. Rev. Lett.* **103**, 015001 (2009).
- [25] See Supplemental Material at <http://link.aps.org/supplemental/10.1103/PhysRevResearch.5.L012030> for additional information, plots, and animations.
- [26] V. Nosenko, M. Pustyl'nik, M. Rubin-Zuzic, A. M. Lipaev, A. V. Zobnin, A. D. Usachev, H. M. Thomas, M. H. Thoma, V. E. Fortov, O. Kononenko, and A. Ovchinin, Shear flow in a three-dimensional complex plasma in microgravity conditions, *Phys. Rev. Res.* **2**, 033404 (2020).
- [27] S. Plimpton, Fast parallel algorithms for short-range molecular dynamics, *J. Comput. Phys.* **117**, 1 (1995).
- [28] J. Hammerberg, D. Lemons, M. Murillo, and D. Winske, Molecular dynamics simulations of plasma crystal formation including wake effects, *IEEE Trans. Plasma Sci.* **29**, 247 (2001).
- [29] P. Ludwig, H. Kählert, and M. Bonitz, Ion-streaming induced order transition in three-dimensional dust clusters, *Plasma Phys. Controlled Fusion* **54**, 045011 (2012).
- [30] D. Kana, C. Dietz, and M. H. Thoma, Simulation of electrorheological plasmas with superthermal ion drift, *Phys. Plasmas* **27**, 103703 (2020).
- [31] See https://github.com/EshitaJoshi/strings_extension for the extension to the LAMMPS code.
- [32] The data generated by the simulation can be found at <https://dx.doi.org/10.5281/zenodo.5845076>.
- [33] T. Antonova, S. A. Khrapak, M. Y. Pustyl'nik, M. Rubin-Zuzic, H. M. Thomas, A. M. Lipaev, A. D. Usachev, V. I. Molotkov, and M. H. Thoma, Particle charge in PK-4 dc discharge from ground-based and microgravity experiments, *Phys. Plasmas* **26**, 113703 (2019).
- [34] G. I. Sukhinin, A. V. Fedoseev, S. N. Antipov, O. F. Petrov, and V. E. Fortov, Dust particle radial confinement in a dc glow discharge, *Phys. Rev. E* **87**, 013101 (2013).
- [35] G. I. Sukhinin, A. V. Fedoseev, M. V. Salnikov, S. N. Antipov, O. F. Petrov, and V. E. Fortov, Influence of ion drag force on radial distribution of dust particles and void formation in a DC glow discharge, *Europhys. Lett.* **103**, 35001 (2013).
- [36] M. Pustyl'nik, A. Pikalev, A. Zobnin, I. Semenov, H. Thomas, and O. Petrov, Physical aspects of dust-plasma interactions, *Contrib. Plasma Phys.* **61**, e202100126 (2021).
- [37] L. Wörner, A. V. Ivlev, L. Couëdel, P. Huber, M. Schwabe, T. Hagl, M. Mikikian, L. Boufendi, A. Skvortsov, A. M. Lipaev, V. I. Molotkov, O. F. Petrov, V. E. Fortov, H. M. Thomas, and G. E. Morfill, The effect of a direct current field on the microparticle charge in the plasma afterglow, *Phys. Plasmas* **20**, 123702 (2013).